Skyrmion clusters and conical droplets in bulk helimagnets with cubic anisotropy

Leonov, A.O.; Pappas, Catherine

Important note
To cite this publication, please use the final published version (if applicable).
Please check the document version above.

Skyrmion clusters and conical droplets in bulk helimagnets with cubic anisotropy

A. O. Leonov[1,2,3,*] and C. Pappas[4,†]

[1]*Chirality Research Center, Hiroshima University, Higashi-Hiroshima, Hiroshima 739-8526, Japan*
[2]*Department of Chemistry, Faculty of Science, Hiroshima University Kagamiyama, Higashi Hiroshima, Hiroshima 739-8526, Japan*
[3]*IFW Dresden, Postfach 270016, 01171 Dresden, Germany*
[4]*Faculty of Applied Sciences, Delft University of Technology, Mekelweg 15, 2629JB Delft, The Netherlands*

Recent experimental findings in the bulk cubic helimagnet and Mott insulator Cu_2OSeO_3 highlight the paramount role of cubic anisotropy in stabilizing novel chiral and skyrmion phases. It was indeed found that if a magnetic field is applied along the easy $\langle 001 \rangle$ crystallographic direction, competing cubic and exchange anisotropies tilt the wave vector of the conical spiral away from the magnetic field [Qian *et al.*, Sci. Adv. **4**, eaat7323 (2018)]. Furthermore, in this configuration skyrmions have been observed in a broad range of temperatures and magnetic fields [Chacon *et al.*, Nat. Phys. **14**, 936 (2018)]. Starting from these experimental observations and on the basis of a phenomenological Dzyaloshinskii theory, we investigate additional implications of the cubic anisotropy for this specified field direction. By including cubic anisotropy we show that the phase transition between the conical and field-polarized or homogeneous states becomes first order. Furthermore, we show that this transition is accompanied by the formation of conical droplets—domains of the conical phase in the homogeneous state. We investigate the internal structure of these droplets, which at their boundaries encompass alternating regions of positive and negative energy densities with respect to the homogeneous state. We thus deduce that these droplets may be zipped and unzipped in phase during the first-order phase transition that occurs by either increasing or decreasing the magnetic field. On the other hand, we show that in the conical phase skyrmions may form clusters due to their attractive mutual interaction. However, in the homogeneous state, the skyrmion-skyrmion interaction becomes repulsive, and the skyrmion clusters expand and disperse isolated skyrmions. This mutual skyrmion repulsion prevents the stabilization of skyrmion clusters even if the energy of isolated skyrmions is lower than that of the homogeneous state. Yet this skyrmion dispersal may be prevented if skyrmions are surrounded by the circular spiral state and form skyrmion bags. Such a scenario could explain the existence of skyrmions in the field-polarized state reported experimentally.

I. INTRODUCTION

At the dawn of skyrmionics [1–3], chiral magnetic skyrmions—topological defects with a complex noncoplanar magnetic structure [4,5]—were first spotted in bulk cubic helimagnets such as the itinerant magnets MnSi [3] and FeGe [6]. In these systems skyrmions appear forming hexagonal lattices in a small pocket of the temperature–magnetic-field phase diagram just below the transition temperature T_C, the so-called A phase. Afterward, the first papers aimed at explaining the stability of chiral skyrmions in the region of the A phase [3,7]. It was found that, within an isotropic phenomenological model, the skyrmion lattice (SkL) is always a metastable solution. However, the energetic difference to its main competitor, the conical phase, is weak and reduces to a minimum for those magnetic fields that stabilize the A phase [8,9]. As a consequence, weak interactions such as the softening of the magnetization modulus [6,10], dipolar interactions, fluctuations [3,11], etc., may modify the energetic landscape and eventually stabilize the SkL in the A-phase pocket. Due to this subtle energetic balance, the boundaries of the A phase can be changed substantially by relatively small external stimuli, such as pressure [12] and electric fields [13–16]. Subsequently, chiral skyrmions (isolated and SkL) have been observed in thin layers of the cubic helimagnets (Fe,Co)Si [17] and FeGe [18] in a broad range of temperatures and magnetic fields. Remarkably, the variable thickness of the layers in these experiments allowed us to tune the region of the A phase from a tiny to a vast area of the temperature–magnetic-field phase diagram.

Generically, the energy differences between the modulated states—helical, conical, and SkL—are small, and thus, the stability regions of these phases and the transitions between them are defined by weak interactions, such as magnetic anisotropy. A remarkable result, however, is that those models that are based on the Dzyaloshinskii theory [19] and include anisotropy show that SkLs should be stabilized over a wide range of magnetic fields and temperatures well beyond the A phase also in bulk cubic helimagnets [4,5,7–9,20]. In particular, uniaxial anisotropy of the easy-axis type [7,8], which does not affect the ideal single-harmonic type of the magnetization rotation in the conical spiral but just leads to the gradual closing of the cone, grants the thermodynamic stability to the SkL in a broad region of a theoretical phase diagram [7–9].

*leonov@hiroshima-u.ac.jp
†c.pappas@tudelft.nl
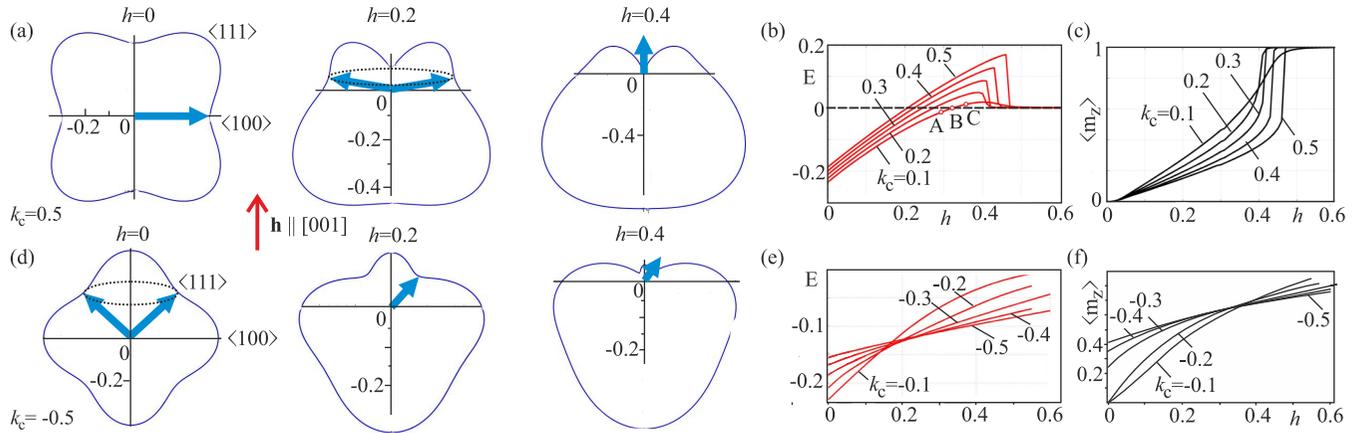
FIG. 1. Energy density obtained by minimizing the energy of the cubic anisotropy (3) and the Zeeman energy for (a) $k_c > 0$ and (d) $k_c < 0$. The energy density of the conical phase with respect to the homogeneous states as a function of the applied magnetic field h for different values k_c of the cubic anisotropy shows that an increasing magnetic field leads to either (b) a FOPT or (b) a second-order PT between the conical and homogeneous states. (c) and (f) The magnetization curves show the component of the magnetization along the field m_z. In (c), $k_c > 0$, and the magnetization jumps into the homogeneous state once it reaches the hard cubic axes $\langle 111 \rangle$ as a consequence of the FOPT. In contrast, in (f) for $k_c < 0$ the magnetization aligns gradually towards the hard axis of $\langle 001 \rangle$, and the transition is second order.

Cubic anisotropy, on the other hand, stabilizes skyrmions even for low temperatures (LTs) but for specific directions of the applied magnetic field. This anisotropy also induces some additional subtle effects because it deforms the ideal conical configuration as the magnetization tends to deviate from the ideal conical surface trying to embrace the easy axes and avoid the hard directions [8,21].

Recently, a new impetus to those theoretical considerations was provided by the reported LT-SkL in the bulk-insulating cubic helimagnet Cu_2OSeO_3 [22,23]. A LT-SkL was shown to be stabilized by cubic anisotropy for a magnetic field applied along [001] [23,24], the easy direction of the cubic anisotropy [8,21]. Additionally, it was shown that the role of cubic anisotropy is not limited to the SkL stability but also leads to many other remarkable phenomena. In particular, the competing effect between the cubic and exchange anisotropies stabilizes a tilted spiral phase [22], which constitutes a major deviation from the generic phase diagram of cubic chiral magnets [3]. This tilted spiral in conjunction with the multiferroic properties of Cu_2OSeO_3 has a strong effect on the magnetically induced electric polarization, affects the spin Hall magnetoresistance [25], and modifies the spin wave spectrum.

The experimental findings hint that cubic anisotropy in Cu_2OSeO_3 also influences the skyrmion nucleation via two different mechanisms [24]: (i) thermodynamically stable skyrmions may appear via rupture formation of *metastable* spiral states with wave vectors perpendicular to the field (in the case of Cu_2OSeO_3 along [100] and [010]); (ii) skyrmions may appear in the form of torons [26] (a localized particle consisting of two Bloch points at finite distance and a convex-shaped skyrmion stretching between them) generated by the inhomogeneous magnetic environment provided by the smooth transition from one tilted spiral domain to another [22].

In the present paper, we focus on additional effects imposed by the cubic anisotropy (excluding its competition

with the exchange anisotropy [22]) in the Mott insulator Cu_2OSeO_3, when the magnetic field is applied along the [001] crystallographic direction. In particular, we examine the stability and structure of dubbed conical droplets, which are generated by the first-order phase transition (FOPT) from the conical phase to the field-polarized state. Experimental phase diagrams (see Fig. 1(c) in Ref. [23] or Fig. 5(c) in Ref. [24]) associate this transition with the field H_{c2}, which we denote by h_B in the theoretical model considered below [Fig. 1(b)]. We also speculate which mechanisms select this particular field direction for skyrmion stabilization [23,24]. The experimental findings [23,24] show that skyrmions exist above this field, and for this reason we also address the stability of skyrmion clusters in the homogeneously magnetized state. In particular, we consider whether skyrmion clusters can be embedded in conical droplets, which stabilize them and preserve their expansion. Finally, we consider the coexistence of skyrmions with the conical state and discuss the stabilization and structure of skyrmion bags, which are skyrmion clusters surrounded by the circular spiral state (CSS) recently introduced in Ref. [27].

II. PHENOMENOLOGICAL MODEL

A. The isotropic micromagnetic energy functional

Our numerical simulations (simulated annealing and a single-step Monte Carlo dynamics with the Metropolis algorithm) are based on the Dzyaloshinskii model for magnetic states in cubic noncentrosymmetric ferromagnets [19,28]:

$$w = (\mathbf{grad\,m})^2 + w_D - \mu_0 M \mathbf{m} \cdot \mathbf{h}. \quad (1)$$

Here, we use reduced values of the spatial variable, $\mathbf{x} = \mathbf{r}/L_D$, where $L_D = A/D$ is the periodicity of the modulated states. A and D are the exchange stiffness and the Dzyaloshinskii constant, respectively, and the sign of D determines the sense of the magnetization rotation; $\mathbf{m} = (\sin\theta\cos\psi; \sin\theta\sin\psi; \cos\theta)$ is the unity vector along

the magnetization vector $\mathbf{M} = \mathbf{m}M$, and $\mathbf{h} = \mathbf{H}/H_D$ with $\mu_0 H_D = D^2/(AM)$ is the applied magnetic field. The energy functional (1) includes only the main interactions necessary to stabilize modulated states. Numerical methods for the energy minimization procedure to obtain solutions for skyrmion clusters and distorted conical states are explicitly described in, e.g., Ref. [29] (Sec. II B).

In the general case of cubic helimagnets, the Dzyaloshinskii-Moriya interaction (DMI) assumes the form [4,19]

$$w_D = \mathcal{L}_{y,z}^{(x)} + \mathcal{L}_{x,z}^{(y)} + \mathcal{L}_{x,y}^{(z)} = \mathbf{m} \cdot \mathrm{rot}\,\mathbf{m} \qquad (2)$$

and includes Lifshitz invariants, $\mathcal{L}_{i,j}^{(k)} = m_i \partial m_j/\partial x_k - m_j \partial m_i/\partial x_k$, along all coordinate axes.

B. Stability of skyrmions in helimagnets with and without the conical phase

The interaction (2) is at the origin of the observed competition between SkL and the conical phase.

To ensure skyrmion stability [8,21] for *bulk* cubic helimagnets, one should supply the model (1) with small anisotropic contributions [7,8], e.g., with the cubic anisotropy $k_c > 0$ (easy $\langle 001 \rangle$ axes) [8,21–23]:

$$w_a = k_c \left(m_x^2 m_y^2 + m_x^2 m_z^2 + m_y^2 m_z^2 \right), \qquad (3)$$

where $k_c = K_c A/D^2$. In the forthcoming sections, we closely examine the underlying mechanisms of such stability for $h||[001]$.

In magnetic *nanolayers* of cubic helimagnets, no anisotropy is needed for skyrmion stability. Indeed, due to $\mathcal{L}_{x,y}^{(z)}$ in (2), the skyrmion helicity changes gradually towards the surfaces. This effect accumulates additional negative energy compared with the cones not decorated by the additional surface twists. Hence, SkL is stabilized in a broad range of applied magnetic fields and nanolayer thicknesses [30–32] even within the model (1) as observed in the first experiments on skyrmion visualization [17,18].

In the C_{nv} [33] and D_{2d} [34] symmetry classes, in contrast, no Lifshitz invariants are present along the high-symmetry z axis, $\mathcal{L}_{x,y}^{(z)}$. Therefore, only modulated magnetic structures with wave vectors perpendicular to the field (i.e., skyrmions and helicoids) are favored by the DMI. These symmetries are exempt from such an ordeal to look for stabilization mechanisms of metastable SkLs. In these materials at the field H_{c1}, thermodynamically *stable* spiral states give rise to the thermodynamically *stable* SkL via formation of merons representing ruptures of a spiral state each with the topological charge $Q = 1/2$ [35,36]. Moreover, Néel (C_{nv}) and antiskyrmions (D_{2d}) are not modified by additional surface twists along z [30]; that is, their physics remains the same in both bulk and nanofabricated magnets.

III. DISTORTED CONICAL PHASE IN THE PRESENCE OF CUBIC ANISOTROPY

A. Solutions for the conical phase with $k_c > 0$ and $k_c < 0$ for $h||[001]$

The equilibrium parameters for the conical phase within the isotropic model (1) are expressed in the analytical

form [28] as

$$\theta_c = \arccos\left(2H/H_D\right), \ \psi_c = z/2L_D. \qquad (4)$$

At the critical field $H = 0.5H_D$, the conical phase of the second-order phase transition transforms into the saturated state with $\theta = 0$.

By including the cubic anisotropy (3) the rotation of the magnetization in the conical phase becomes in tune with a complex energy landscape with various global and local minima. For $k_c > 0$ and $h = 0$ [Fig. 1(a)], the magnetization in the conical phase (blue arrow) rotates in the plane (001). While rotating, the magnetization leaves one energy minimum of (3) corresponding to a $\langle 001 \rangle$ direction and, rotating through the saddle point between hard $\langle 111 \rangle$ axes, gets into another energy minimum. In the applied magnetic field, the magnetization in the conical phase is forced to rotate in the environment of hard $\langle 111 \rangle$ axes [Fig. 1(a), $h = 0.2, 0.4$] that underlie the subsequent FOPT into the homogeneous state [Figs. 1(b) and 1(c)].

For $k_c < 0$ and $h = 0$ [Fig. 1(d)], the equilibrium states of the energy functional (3) correspond to the easy axes of cubic anisotropy oriented along $\langle 111 \rangle$ crystallographic directions. The angle of this easy direction with respect to the field $h||[001]$ is $70.5°$. Maxima of the functional (3) are $\langle 001 \rangle$ directions: the hard axes of cubic anisotropy. The magnetization in the conical phase performs such a rotation to sweep the easy directions $\langle 111 \rangle$. Even in zero field the conical phase has a nonzero component of the magnetization along the field [see magnetization curves in Fig. 1(f)]. In the applied magnetic field the global minima of Eq. (3) gradually approach the field direction and thus display the second-order phase transition toward the homogeneous state [Figs. 1(e) and 1(f)]. The same principles are valid also for $\mathbf{h}||[111]$. For example, for $k_c > 0$, the phase transition remains second order—the magnetization in the conical phase that embraces easy $\langle 001 \rangle$ axes gradually aligns along the hard direction [111] with increasing magnetic field. The exquisite information on the structure of all modulated structures in the presence of the cubic anisotropy and the corresponding theoretical phase diagrams are presented in Refs. [8,21,24].

The stabilization effect of cubic anisotropy on SkL becomes apparent for the cases of FOPT between the cones and the homogeneous state [8,21,23]. The strategy of SkL stabilization by the cubic anisotropy is quite the opposite of that used in nanolayers [30]. In nanolayers due to the surface twists [30,31,37], the SkLs possess additional negative energy [32] compared with the unchanged energy of the conical phase without the surface twists. The cubic anisotropy in bulk magnets is rather invoked to distort both SkL and the cone, but with a much stronger impact on the cone for particular directions of the field. In the following, we will focus on some effects that appear at low temperatures when the system undergoes a FOPT from the conical to the field-polarized state.

B. Conical droplets

During the FOPT realized for $k_c > 0$ and $h||[001]$, droplets of the conical phase may persist in the field-polarized state, adopting the configuration illustrated in Fig. 2. Such domains
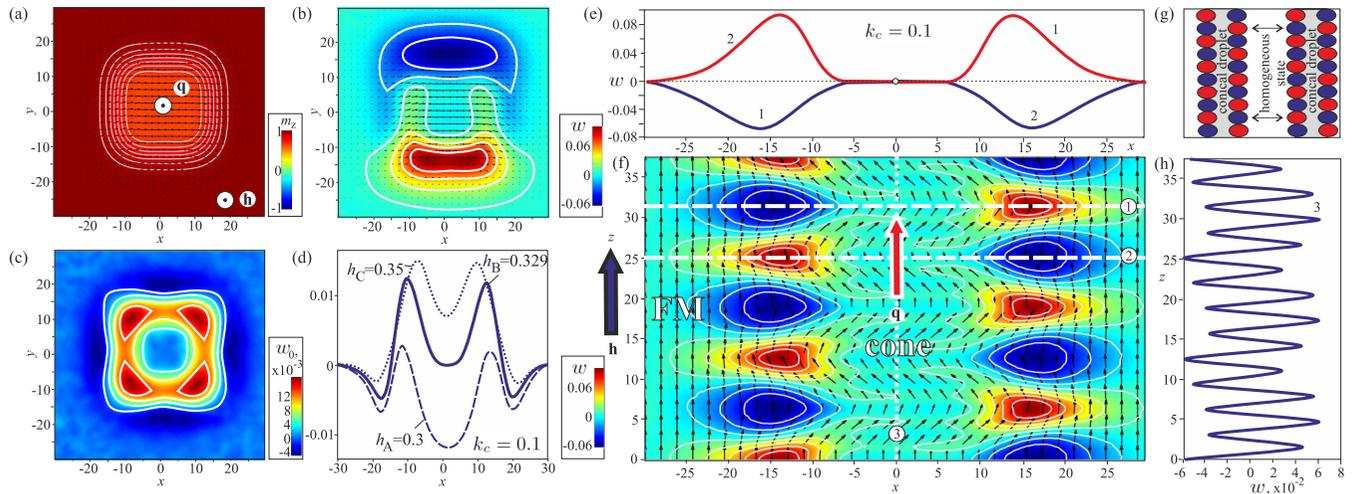
FIG. 2. Internal structure of conical droplets formed during the FOPT from the conical state to the homogenous state, shown as color plots of (a) the magnetization and (b) the energy density w. The black arrows are projections of the magnetization onto the xy plane. The $\mathbf{q}$ vector of the conical phase and the applied magnetic field $\mathbf{h}$ are directed along z. (c) The energy density w_0 averaged over the cone period is shown as a color plot in the xy plane with (d) its cross sections for three values of the field, corresponding to the FOPT at h_B (solid blue line), below FOPT h_A (dashed line), and above FOPT h_C (dotted line). (f) The energy density in the xz cross section of the conical droplet exhibits alternating parts with the negative and positive contributions corresponding to correct and wrong senses of the magnetization rotation at the boundary to the FM state. (e) The corresponding linear cross sections along x marked by dashed lines 1 and 2 in (f). (h) A linear cross section along z marked by dotted line 3 in (f). (g) Schematic representation of the in-phase zipping and unzipping of conical droplets (see text for details).

exhibit both types of the rotational sense at their boundaries. At the upper side of the depicted conical droplet [Fig. 2(a)] the magnetization in the conical phase adjusts to the homogeneous state with the "correct" twist supported by the DMI (2). This leads to the energy gain shown by the negative energy density plotted in the xy plane [Fig. 2(b)], i.e., for a cross section perpendicular to the magnetic field $\mathbf{h}$ and the conical $\mathbf{q}$ vector. On the lower side of the conical droplet, the magnetization acquires the "wrong" in-plane twist, which results in an energetic "penalty" [Fig. 2(b)].

A similar behavior is also found along the z direction, which is parallel to $\mathbf{h}$ and $\mathbf{q}$. As illustrated in Fig. 2(f), the energy density of the conical droplet exhibits alternating negative and positive contributions corresponding to correct and wrong senses of the magnetization rotation at the boundary to the field-polarized state. In addition, as a consequence of the easy and hard axes imposed by the cubic anisotropy, the magnetization at the droplet core slightly deviates from the optimal conical angle, as shown in Fig. 2(h). The energy density w_0 averaged over the cone period [Fig. 2(c)] shows that the conical droplet is surrounded by a ring of negative energy density [Fig. 2(d)]. The core with the conical phase has about the same energy density as the homogeneous state and is surrounded by a ring with positive energy density. When the magnetic field is increased from the conical to the homogeneous phase, the conical droplet may either continuously expand for $h < h_B$, as seen in Fig. 1(b), or gradually shrink for $h > h_B$, a feature that underlies the kinetic character of such FOPT. Remarkably, when the magnetic field is decreased from the field-polarized to the conical state, the energy density shown in Fig. 2(f) leads to an "in-phase" merger of neighboring conical droplets that initially may be formed with some phase shift with respect to each other. Then, the region with the positive energy density at the boundary

of one conical droplet is annihilated by the corresponding part with the negative energy of another droplet, a feature that underlies in-phase "zipping" and "unzipping" of conical droplets [schematically shown in Fig. 2(g)].

IV. SKYRMION CLUSTERS AND BAGS

A. Skyrmion clusters as initiators of FOPT from the conical to the homogeneous state

First, we justify that within our model we deal with skyrmion clusters and not with the extended SkL. Within the theoretical framework, SkL represents a hexagonal lattice of closely packed skyrmions: such a state is usually numerically addressed by considering two skyrmions in a cell with periodic boundary conditions. By skyrmion clusters we imply a group of skyrmions surrounded by the conical (homogeneous) states.

As known, e.g., from Refs. [22,23,38], the zero-field state of Cu_2OSeO_3 represents domains of helical spirals with the magnetic moments rotating in the {001} planes and the $\mathbf{q}$ vectors propagating along the three equivalent ⟨001⟩ crystallographic directions. An applied magnetic field, $\mathbf{h}||[001]$, induces the conical state, where the state with the helical propagation vector along the magnetic field corresponds to the global energetic minimum, whereas the helices along the other directions become metastable solutions. Such metastable spiral domains, however, may give rise to the thermodynamically stable skyrmions [24,35,36], which therefore form clusters within the conical state. These would be nonaxisymmetric skyrmions similar to those that were recently introduced theoretically in Refs. [39,40] and observed experimentally in thin layers of Cu_2OSeO_3 [37]. These skyrmions are incompatible with the conical phase and are thus surrounded by a circlelike shell, which is a transitional region with positive energy that
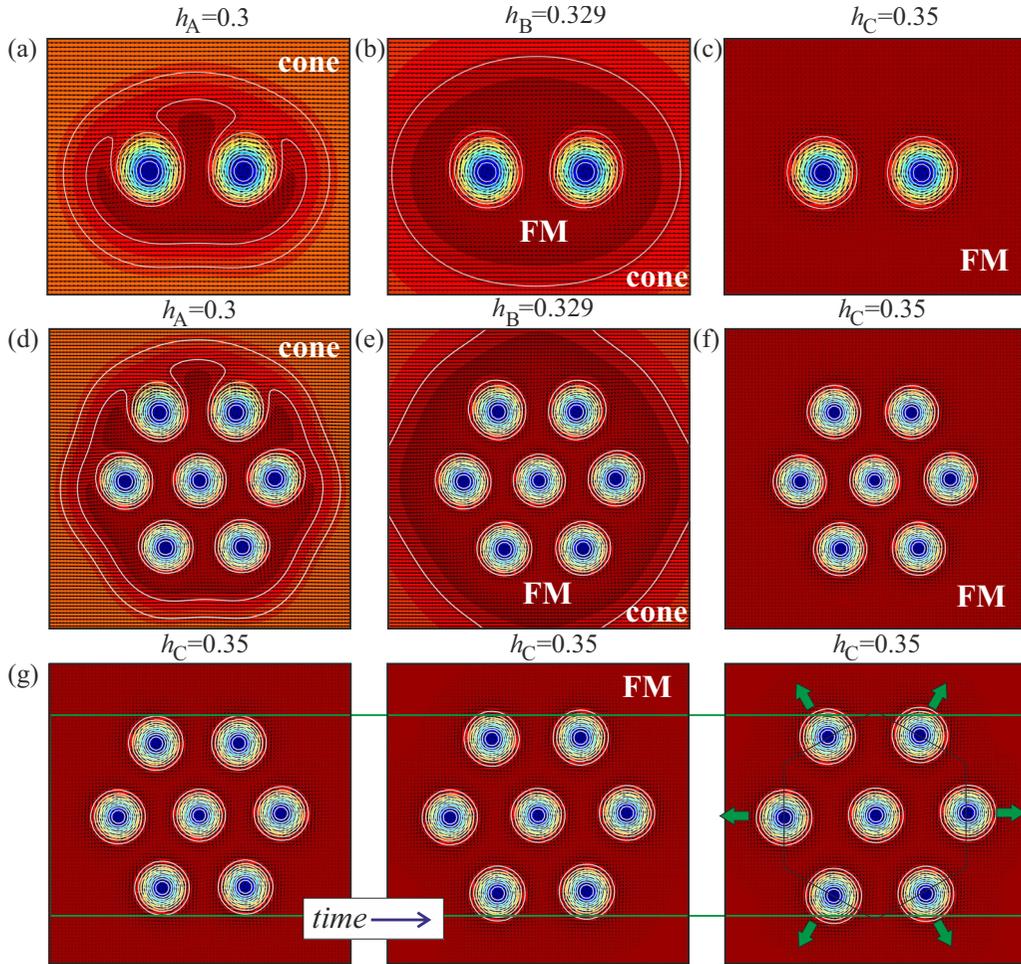
FIG. 3. Skyrmion clusters consisting of (a)–(c) two and (d)–(f) seven skyrmions surrounded by (a) and (d) the conical phase for $h < h_B$ and (b) and (e) initiating FOPT into the FM state for $h = h_B$. (c), (f), and (g) At $h > h_B$ the isolated skyrmions due to the repulsive interskyrmion potential continue to move away from each other. In (g) such an expansion is shown for a fixed value of the field $h_C = 0.35$, $k_c = 0.1$. The green lines and arrows in (f) are shown as a guide for the eye.

underlies the attractive interskyrmion potential and leads to skyrmion cluster formation [39,40].

With increasing magnetic field, it is reasonable to expect that these skyrmion clusters persist up to the FOPT between the conical and homogeneous states, where they may be encompassed by conical droplets and form skyrmion bags. This would explain the experimental phase diagrams and the SkL stability regions exceeding the H_{c2} field [23,24].

Our findings, however, indicate a different evolution because the energy density at the boundary (shell) between skyrmions and the conical phase is much higher than the one between conical droplets and the homogeneous state. Thus, the FOPT and the onset of the homogeneous state modifies the skyrmion internal structure, which becomes axisymmetric. Figure 3(a) shows a pair of attracted skyrmions for the field $h_A = 0.3$ below the FOPT. For $h = h_B$ the skyrmion pair becomes surrounded by the homogeneous state, and the interskyrmion attraction turns into a repulsion [41] [Fig. 3(b)]. The expanding homogeneous state eventually occupies the whole space [Fig. 3(c)]. This scenario applies independently of the number of skyrmions in a cluster [Figs. 3(d)–3(f)].

Due to the repulsive skyrmion-skyrmion interaction within the homogeneous state, the FOPT is accompanied by the subsequent dispersal of isolated skyrmions. Figure 3(g) shows gradual expansion of a skyrmion cluster for a fixed value of the field. It is thus impossible to contain skyrmion clusters in the saturated state. These considerations are also based on the experimental observations of skyrmion clusters in thin (70 mn) single-crystal samples of Cu_2OSeO_3 by transmission electron microscopy [37], although these experiments were not able to unambiguously identify the conical phase in the featureless regions of the images that surround the skyrmion clusters. Nevertheless, the fact that skyrmions form clusters already by itself indirectly indicates that the interaction between these skyrmions should be attractive [37].

B. Skyrmion clusters surrounded by the circular spiral state: Skyrmion bags

Skyrmion clusters within the homogeneous state may, however, be created if multiple skyrmions are nested within a region surrounded by the CSS, the situation possible in the experiments on Cu_2OSeO_3. Indeed, the metastable spiral
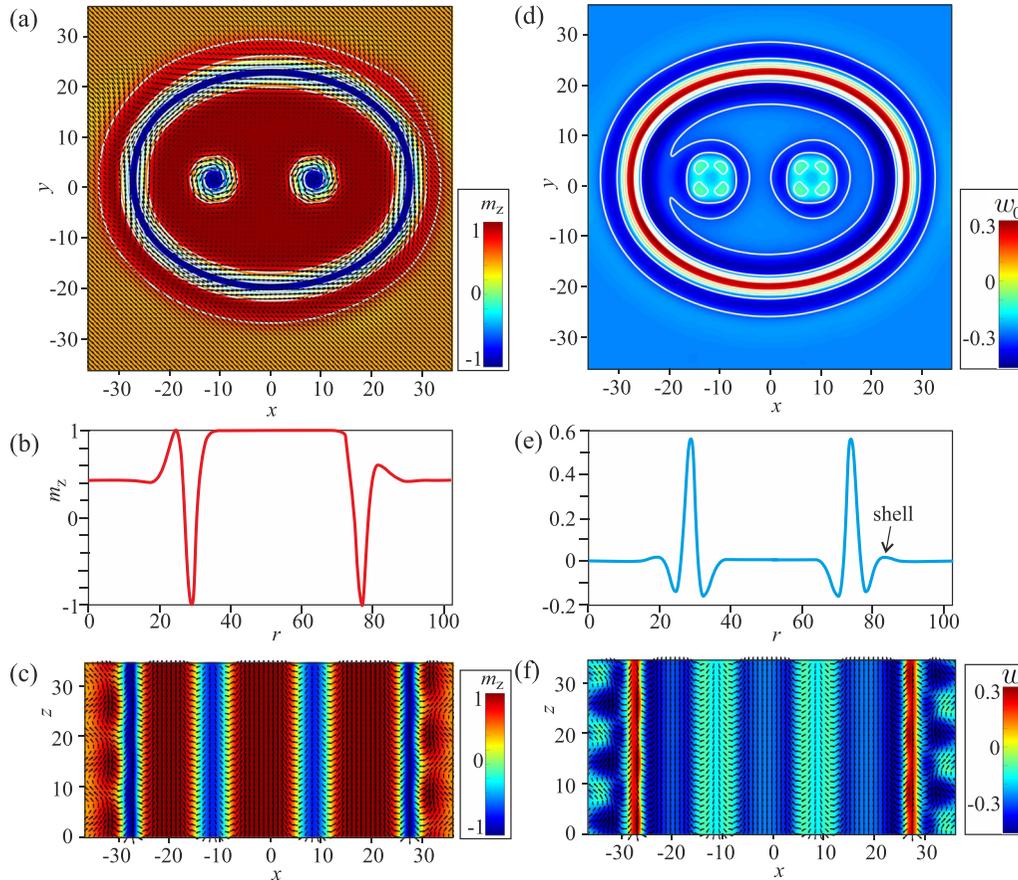
FIG. 4. Skyrmion bag that contains two skyrmions with the total topological charge $Q = -2$. (a) and (c) The color plots indicate the z component of the magnetization, and the black arrows are projections of the magnetization onto the xy and xz planes, respectively. (d) Energy density w_0 averaged over the cone period is plotted on the xy plane. (f) Energy density w (1) is plotted on the plane xz. (b) and (e) Curves show diagonal cross sections of upper color plots excluding skyrmions. In particular, (e) indicates the outer region of the shell with the positive energy density introduced in Refs. [37,39,40] that underlies an attractive interaction.

domains may form the boundary with respect to the conical phase in the form of a CSS rather than in the form of merons that would cost more energy. This also creates prerequisites that such a CSS will not give rise to skyrmions and at the field H_{c1} will surround a skyrmion cluster. Such a concept of so-called skyrmion bags was recently theoretically suggested in Ref. [27] and experimentally observed in chiral liquid crystals [27]. In the skyrmion bags (which in a particular case contain just two skyrmions; Fig. 4), the repulsive interaction between skyrmions is counteracted by the positive energy density of the encompassing CSS; that is, one optimizes two length scales: the distance between skyrmions and the length of the surrounding CSS.

The structure of such skyrmion bags is closely related to the structure of skyrmion clusters stabilized in nanodisks or nanowires [42–44]. The surface area of a nanowire cross section defines the number of skyrmions in the cluster and their characteristic sizes. Moreover, the skyrmions are confined by the circular edge states spontaneously formed at the wire boundaries. Such edge states repulse skyrmions but still enable their field-driven escape from a wire. An edge state represents just a part of considered CSS (Fig. 4) with the magnetization rotation up to some critical angle that ensures its negative energy density [42].

Remarkably, a skyrmion bag placed into the conical phase maintains the homogeneous state inside, whereas the outer side of the CSS forms a complex domain boundary with the surrounding conical phase (shell [37,39,40]). Obviously, the formation of the shell between the inner side of the CSS and the conical phase as well as the shell between skyrmions and the conical phase is energetically unfavorable. Thus, the CSS may subdivide the space into regions with repulsive (inner space) and attractive (outer space) interskyrmion potential.

For magnetic nanowires with small radii, the aforementioned arguments will also hold, and skyrmions will be surrounded by the homogeneous state. For larger nanowire diameters, however, the conical phase will also be formed in the nanowire cross section. The energy loss due to the shell formation between the conical phase and skyrmion clusters as well as due to the complex structure of edge states will be outbalanced by the energy gain due to regions occupied by the conical phase. Such a crossover from repulsive to attractive skyrmion interaction is expected to be a function of a nanowire radius and skyrmion number in a cluster, a concept to be proven experimentally.

Thus, we attribute the experimental observation of the SkL signal in bulk samples of Cu_2OSeO_3 for fields exceeding H_{c2} [23,24] to the following: the interskyrmion repulsion

is very weak, and thus, the skyrmion clusters may locally preserve the hexagonal order, which is captured by experiments with gradually increasing magnetic field; this may be additionally influenced by the lattice pinning. We also do not exclude the existence of skyrmion bags, the formation of which is stipulated by the high energy of the boundary between the conical phase and skyrmions. Remarkably, the extended skyrmion lattice may exist well above the field H_{c2} (see, e.g., the theoretical phase diagram in Fig. 30 of Ref. [21] or Fig. 7(a) of Ref. [24]). Then, the additional skyrmions must be nucleated within the conical phase (possibly via toron elongation [26]) to complement already existing skyrmions in the clusters and thus to fill the whole space. All described theoretical concepts should be revisited by new, carefully devised experiments.

V. CONCLUSIONS

In conclusion, we considered the internal structure of domains of the conical phase that appear during the first-order phase transition with the field-saturated state in bulk cubic helimagnets. We found that the boundary formed between the conical and homogeneous states exhibits two rotational senses and thus acquires positive or negative energy density

that underlies the in-phase zipping and unzipping of conical droplets. The skyrmion clusters within the conical phase were shown to initiate the first-order phase transition into the homogeneous state since the skyrmions first get rid of the energetically costly boundary with respect to the conical phase. We argue that due to the repulsive interskyrmion potential in the homogeneous state no skyrmion clusters are possible. We also examine the structure of so-called skyrmion bags surrounded by the conical phase. Whereas the conical phase could form a boundary with the circular spiral state underlying attracting interaction, it could not penetrate the interior of the bag, leaving skyrmions to repulse each other. Taking into account the scenario of skyrmion nucleation from the domains of spiral states, the skyrmion bags could also be formed in Cu_2OSeO_3.

[1] K. Kadowaki, K. Okuda, and M. Date, J. Phys. Soc. Jpn **51**, 2433 (1982).

[2] Y. Ishikawa and M. Arai, J. Phys. Soc. Jpn. **53**, 2726 (1984).

[3] S. Mühlbauer, B. Binz, F. Jonietz, C. Pfleiderer, A. Rosch, A. Neubauer, R. Georgii, and P. Böni, Science **323**, 915 (2009).

[4] A. N. Bogdanov and D. A. Yablonskii, Zh. Eksp. Teor. Fiz. **95**, 178 (1989) [Sov. Phys. JETP **68**, 101 (1989)].

[5] A. Bogdanov and A. Hubert, J. Magn. Magn. Mater. **138**, 255 (1994); **195**, 182 (1999).

[6] H. Wilhelm, M. Baenitz, M. Schmidt, U. K. Rößler, A. A. Leonov, and A. N. Bogdanov, Phys. Rev. Lett. **107**, 127203 (2011).

[7] A. B. Butenko, A. A. Leonov, U. K. Rößler, and A. N. Bogdanov, Phys. Rev. B **82**, 052403 (2010).

[8] A. A. Leonov, Ph.D. thesis, Technical University of Dresden, 2012.

[9] M. N. Wilson, A. B. Butenko, A. N. Bogdanov, and T. L. Monchesky, Phys. Rev. B **89**, 094411 (2014).

[10] A. O. Leonov and A. N. Bogdanov, New J. Phys. **20**, 043017 (2018).

[11] S. Buhrandt and L. Fritz, Phys. Rev. B **88**, 195137 (2013).

[12] I. Levatic, P. Popcevic, V. Surija, A. Kruchkov, H. Berger, A. Magrez, J. S. White, H. M. Ronnow, and I. Zivkovic, Sci. Rep. **6**, 21347 (2016).

[13] Y. Okamura, F. Kagawa, S. Seki, and Y. Tokura, Nat. Commun. **7**, 12669 (2016).

[14] J. S. White, K. Prsa, P. Huang, A. A. Omrani, I. Zivkovic, M. Bartkowiak, H. Berger, A. Magrez, J. L. Gavilano, G. Nagy *et al.*, Phys. Rev. Lett. **113**, 107203 (2014).

[15] A. J. Kruchkov, J. S. White, M. Bartkowiak, I. Zivkovic, A. Magrez, and H. M. Ronnow, Sci. Rep. **8**, 10466 (2018).

[16] J. S. White, I. Zivkovic, A. J. Kruchkov, M. Bartkowiak, A. Magrez, and H. M. Ronnow, Phys. Rev. Appl. **10**, 014021 (2018).

[17] X. Z. Yu, Y. Onose, N. Kanazawa, J. H. Park, J. H. Han, Y. Matsui, N. Nagaosa, and Y. Tokura, Nature (London) **465**, 901 (2010).

[18] X. Z. Yu, N. Kanazawa, Y. Onose, K. Kimoto, W. Z. Zhang, S. Ishiwata, Y. Matsui, and Y. Tokura, Nat. Mater. **10**, 106 (2011).

[19] I. E. Dzyaloshinskii, J. Exp. Theor. Phys. **19**, 960 (1964); **20**, 223 (1965); **20**, 665 (1965).

[20] U. K. Roessler, A. N. Bogdanov, and C. Pfleiderer, Nature (London) **442**, 797 (2006).

[21] A. Leonov, arXiv:1406.2177.

[22] F. Qian, L. J. Bannenberg, H. Wilhelm, G. Chaboussant, L. M. DeBeer-Schmitt, M. P. Schmidt, A. Aqeel, T. T. M. Palstra, E. H. Bruck, A. J. E. Lefering, C. Pappas, M. Mostovoy, and A. O. Leonov, Sci. Adv. **4**, eaat7323 (2018).

[23] A. Chacon, L. Heinen, M. Halder, A. Bauer, W. Simeth, S. Mühlbauer, H. Berger, M. Garst, A. Rosch, and C. Pfleiderer, Nat. Phys. **14**, 936 (2018).

[24] L. J. Bannenberg, H. Wilhelm, R. Cubitt, A. Labh, M. Schmidt, E. Lelievre-Berna, C. Pappas, M. Mostovoy, and A. O. Leonov, NPJ Quantum Mater. **4**, 11 (2019).

[25] A. Aqeel, N. Vlietstra, A. Roy, M. Mostovoy, B. J. van Wees, and T. T. M. Palstra, Phys. Rev. B **94**, 134418 (2016).

[26] A. O. Leonov and K. Inoue, Phys. Rev. B **98**, 054404 (2018).

[27] D. Foster, C. Kind, P. J. Ackerman, J.-S. B. Tai, M. R. Dennis, and I. I. Smalyukh, Nat. Phys. (2019), doi:10.1038/s41567-019-0476-x.

[28] P. Bak and M. H. Jensen, J. Phys. C **13**, L881 (1980).

[29] A. O. Leonov and I. Kezsmarki, Phys. Rev. B **96**, 214413 (2017).

[30] A. O. Leonov, Y. Togawa, T. L. Monchesky, A. N. Bogdanov, J. Kishine, Y. Kousaka, M. Miyagawa, T. Koyama, J. Akimitsu, Ts. Koyama, K. Harada, S. Mori, D. McGrouther, R. Lamb, M. Krajnak, S. McVitie, R. L. Stamps, and K. Inoue, Phys. Rev. Lett. **117**, 087202 (2016).

[31] S. L. Zhang, G. van der Laan, W. W. Wang, A. A. Haghighirad, and T. Hesjedal, Phys. Rev. Lett. **120**, 227202 (2018).

[32] D. McGrouther, R. J. Lamb, M. Krajnak, S. McFadzean, S. McVitie, R. L. Stamps, A. O. Leonov, A. N. Bogdanov, and Y. Togawa, New J. Phys. **18**, 095004 (2016).

[33] S. Bordacs, A. Butykai, B. G. Szigeti, J. S. White, R. Cubitt, A. O. Leonov, S. Widmann, D. Ehlers, H.-A. Krug von Nidda, V. Tsurkan, A. Loidl, and I. Kezsmarki, Sci. Rep. **7**, 7584 (2017).

[34] A. K. Nayak, V. Kumar, P. Werner, E. Pippel, R. Sahoo, F. Damay, U. K. Roessler, C. Felser, and S. S. P. Parkin, Nature (London) **548**, 561 (2017).

[35] J. Müller, J. Rajeswari, P. Huang, Y. Murooka, H. M. Ronnow, F. Carbone, and A. Rosch, Phys. Rev. Lett. **119**, 137201 (2017).

[36] A. O. Leonov, A. N. Bogdanov, and K. Inoue, Phys. Rev. B **98**, 060411(R) (2018).

[37] J. C. Loudon, A. O. Leonov, A. N. Bogdanov, M. C. Hatnean, and G. Balakrishnan, Phys. Rev. B **97**, 134403 (2018).

[38] S. Seki, X. Z. Yu, S. Ishiwata, and Y. Tokura, Science **336**, 198 (2012).

[39] A. O. Leonov, J. C. Loudon, and A. N. Bogdanov, Appl. Phys. Lett. **109**, 172404 (2016).

[40] A. O. Leonov, T. L. Monchesky, J. C. Loudon, and A. N. Bogdanov, J. Phys.: Condens. Matter **28**, 35LT01 (2016).

[41] A. O. Leonov, T. L. Monchesky, N. Romming, A. Kubetzka, A. N. Bogdanov, and R. Wiesendanger, New J. Phys. **18**, 065003 (2016).

[42] A. O. Leonov, U. K. Roessler, and M. Mostovoy, EPJ Web Conf. **75**, 05002 (2014).

[43] F. Zheng, H. Li, S. Wang, D. Song, C. Jin, W. Wei, A. Kovacs, J. Zang, M. Tian, Y. Zhang, H. Du, and R. E. Dunin-Borkowski, Phys. Rev. Lett. **119**, 197205 (2017).

[44] X. Zhao, C. Jin, C. Wang, H. Du, J. Zang, M. Tian, R. Che, and Y. Zhang, Proc. Natl. Acad. Sci. USA **113**, 4918 (2016).